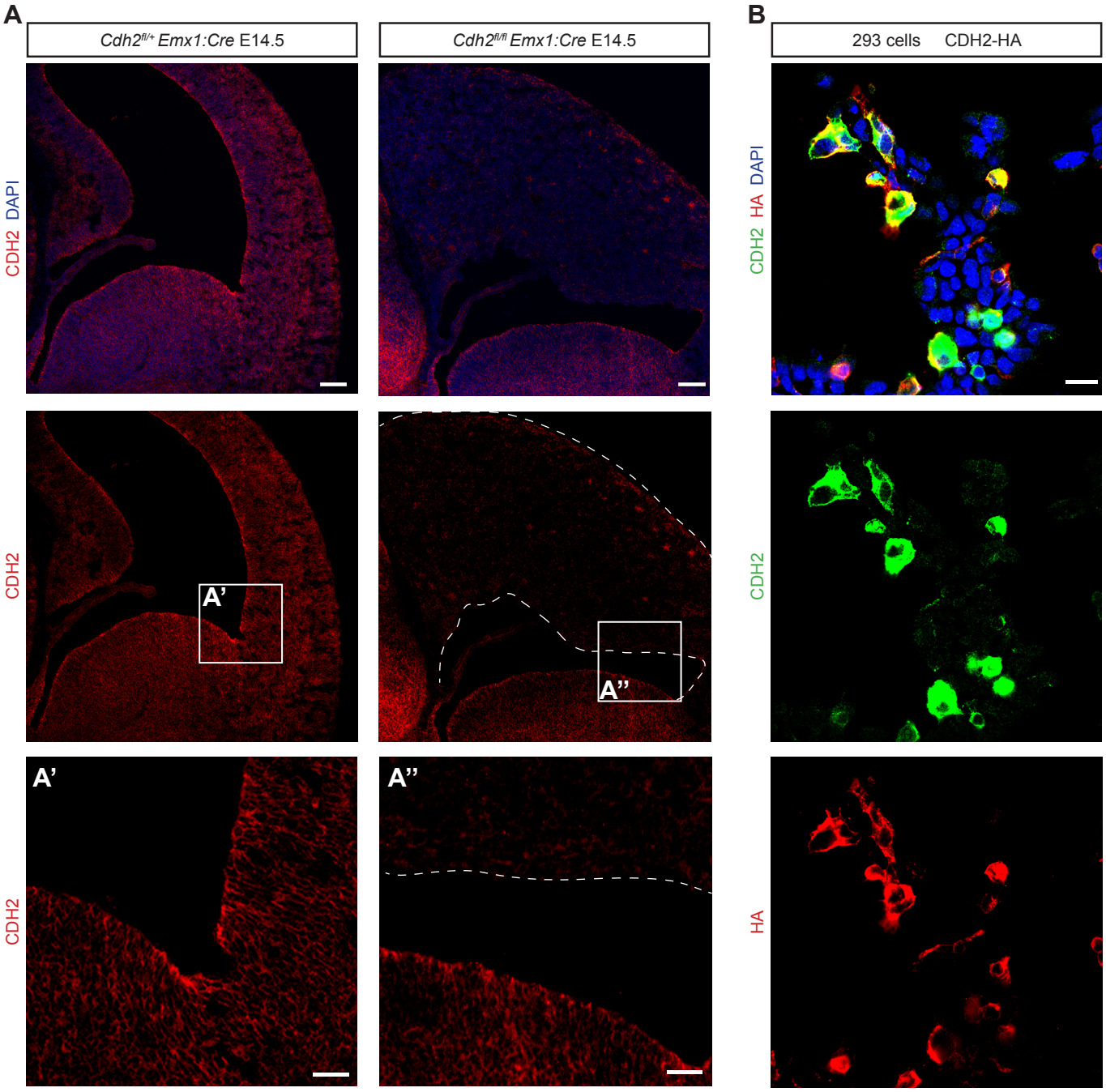

Fig. S1. Specificity of anti-CDH2 antibody. (**A**) E14.5 brains from *Cdh2*$^{fl/+}$ *Emx1:Cre* or *Cdh2*$^{fl/fl}$ *Emx1:Cre* mice were stained with anti-CDH2 (6B3) rat monoclonal antibody obtained from the Hybridoma Bank. CDH2 staining is greatly decreased in the cortex of *Cdh2*$^{fl/fl}$ *Emx1:Cre* animals (A'', delimited by dotted lines), but remains unaffected in the ventral pallium (where Cre is not expressed) and in *Cdh2*$^{fl/+}$ *Emx1:Cre* mice (A', A''). Nuclei are counterstained with DAPI (blue). (**B**) 293 cells transfected with an HA-tagged CDH2 protein were double stained with anti-HA and anti-CDH2 antibodies. Green (CDH2) and red (HA) signals colocalize in all transfected cells. Nuclei are counterstained with DAPI (blue). Scale bars: 100 μm (A); 50 μm (A', A''); 20 μm (B).

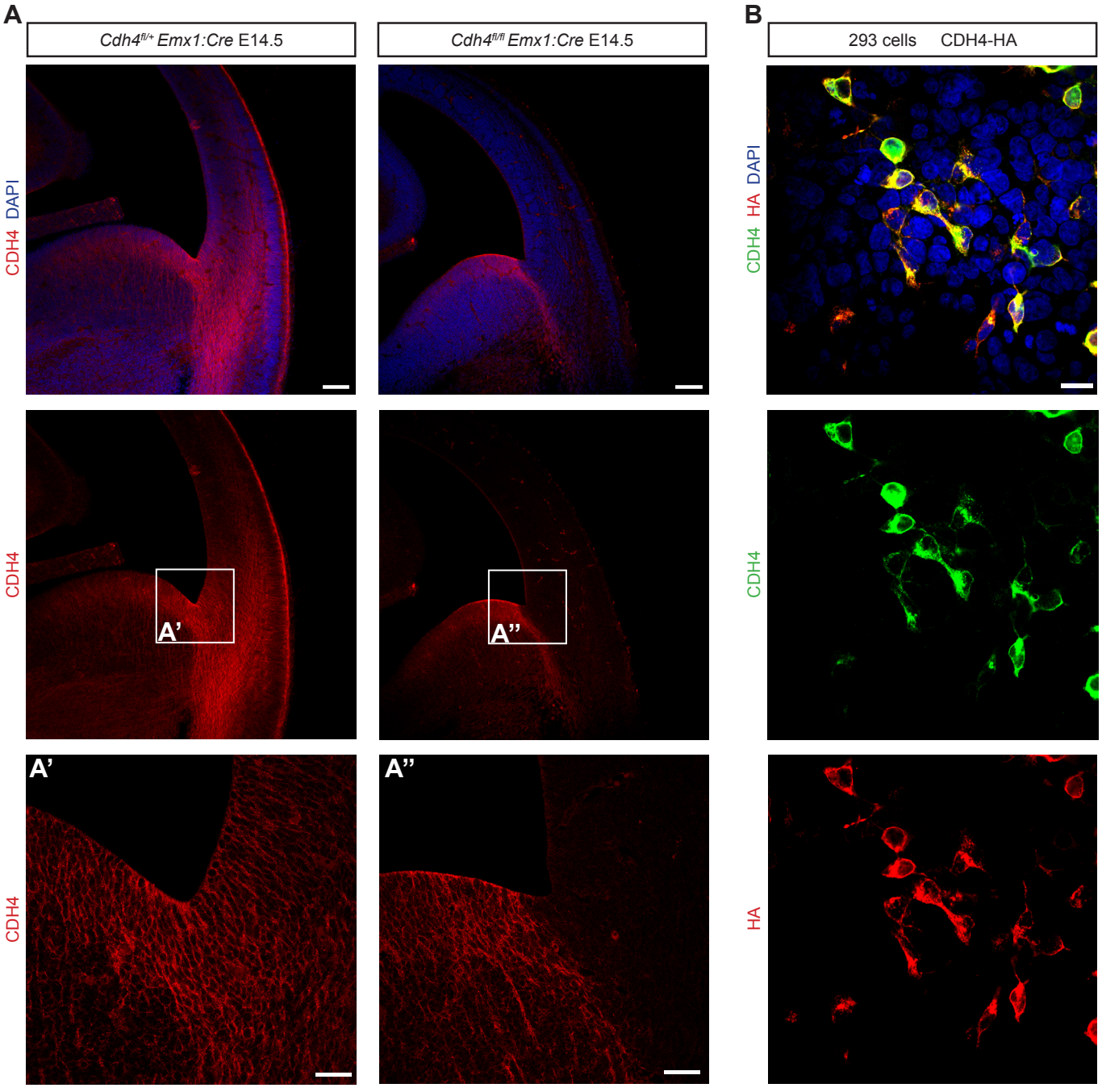

Fig. S2. Specificity of anti-CDH4 antibody. (**A**) E14.5 brains from *Cdh4*$^{fl/+}$ *Emx1:Cre* or *Cdh4*$^{fl/fl}$ *Emx1:Cre* mice were stained with anti-CDH4 (MRCD5) rat monoclonal antibody obtained from the Hybridoma Bank. CDH4 staining is greatly decreased in the cortex of *Cdh4*$^{fl/fl}$ *Emx1:Cre* animals (A''), but remains unaffected in the ventral pallium (where Cre is not expressed) and in *Cdh4*$^{fl/+}$ *Emx1:Cre* mice (A', A''). Nuclei are counterstained with DAPI (blue). (**B**) 293 cells transfected with an HA-tagged CDH4 protein were double stained with anti-HA and anti-CDH4 antibodies. Green (CDH4) and red (HA) signals colocalize in all transfected cells. Nuclei are counterstained with DAPI (blue). Scale bar: 100 μm (A); 50 μm (A', A''); 20 μm (B).

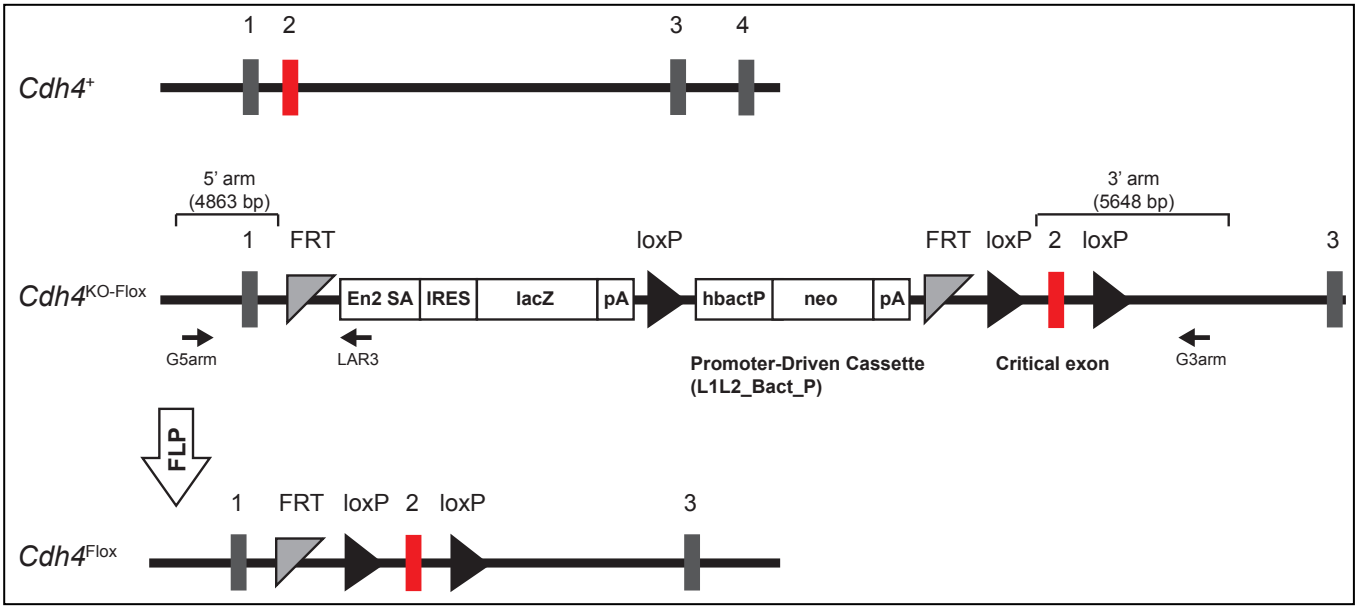

Fig. S3. Generation of *Cdh4*^{cko} mice. Schematic diagram of wild type, knock-out first mutation and floxed (flox) alleles of the *Cdh4* gene. The "knock-out first" allele from EUCOMM contains a targeting construct within intron 1 of the gene. This construct comprises an IRES:lacZ trappig cassette and a floxed promoter-driven neo cassette for selection. An Engrailed (En2) splice acceptor site 5' of the IRES:lacZ cassette disrupts gene function and generates a LacZ fusion protein to study gene expression. Recombination between the two FRT sites, mediated by Flp recombinase, removes the gene trap cassette and creates a conditional allele (flox) (modified from (Ryder et al., 2013) and (Gil-Sanz et al., 2013)). Exons are depicted as numbered boxes, with the floxed exon shown in red. PCR primers for genotyping (G5arm, G3arm, and LAR3) are indicated.

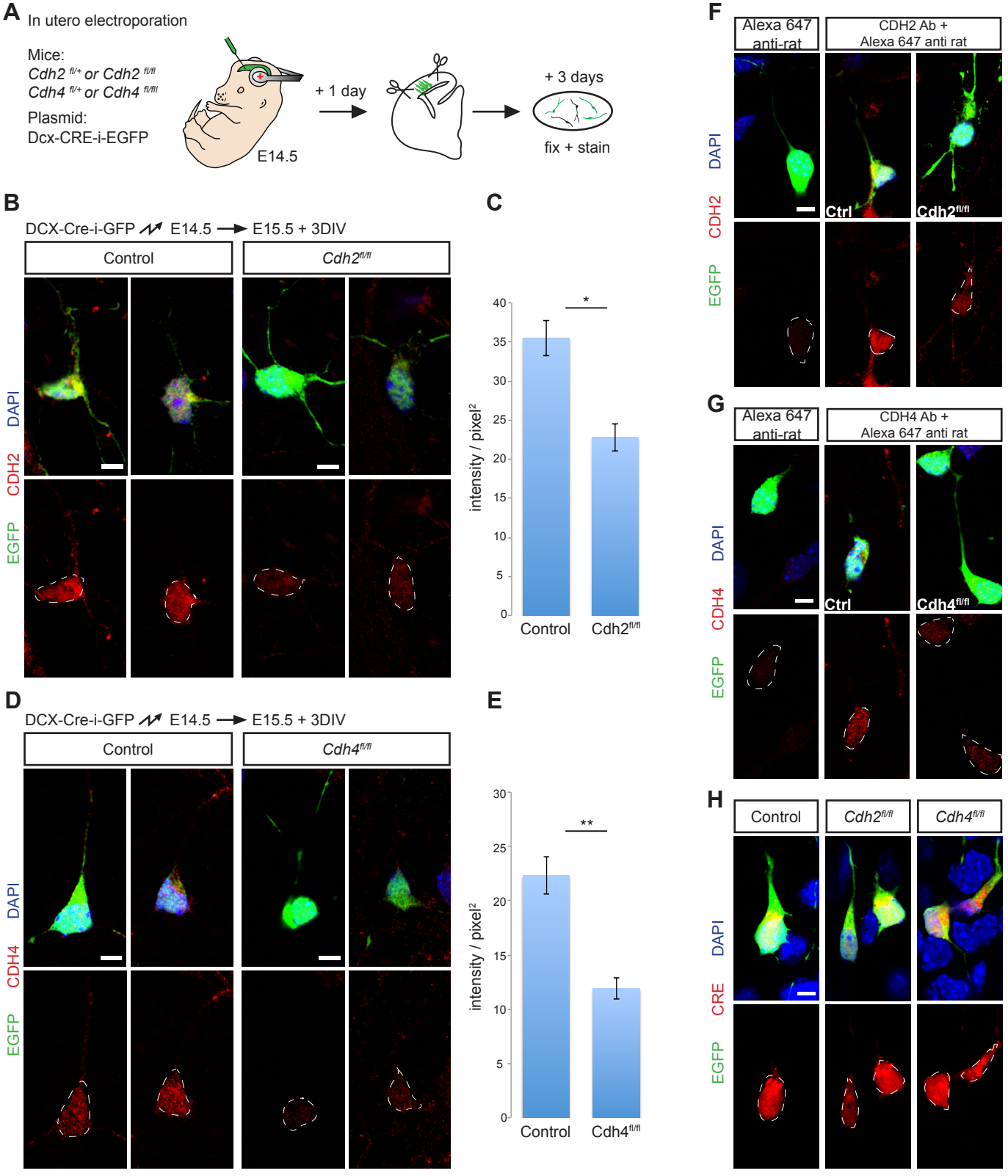

Fig. S4. Cadherin2/4 reduction after Cre electroporation. (**A**) Diagram of experimental strategy to analyze protein reduction after Cre electroporation into floxed animals. E14.5 control, $Cdh2^{fl/fl}$ or $Cdh4^{fl/fl}$ animals were electroporated with a plasmid driving Cre expression from the Doublecortin promotor. One day after electroporation, cortices were dissociated and neurons cultured in vitro for a further 3 days before fixation and staining with specific antibodies. (**B**) Representative images of control and $Cdh2^{fl/fl}$ Cre-electroporated neurons stained with anti-CDH2 antibody. Electroporated neurons are identified by EGFP expression (green). CDH2 (red) intensity is significantly reduced in the targeted cells. (**C**) Quantification of the data in (B). After 4 days, CDH2 levels are reduced by about 36% compared to control neurons. *$p < 0.001$ by Student's t test. Measurements were performed on 10 cells from two separate experiments for each condition. (**D**) Representative images of control and $Cdh4^{fl/fl}$ Cre-electroporated neurons stained with anti-CDH4 antibody. Again, EGFP expression (green) identifies targeted cells. The intensity of CDH4 (red) staining is significantly reduced in the floxed neurons. (**E**) Quantification of the data in (D). 4 days after electroporation, CDH4 levels are reduced by 47% compared to control neurons. **$p < 0.0001$ by Student's t test. Measurements were performed on 10 and 11 cells from two separate experiments for control and $Cdh4^{fl/fl}$, respectively. (**F** and **G**) Secondary antibody controls for the CDH2 and CDH4 stainings. In the absence of primary antibody, no cadherin signal (red) can be detected. (H) Control for Cre expression in targeted cells. Electroporated neurons from control, $Cdh2^{fl/fl}$ or $Cdh4^{fl/fl}$ animals were stained with anti-Cre antibody. All EGFP expressing cells (green) show strong Cre expression (red). In all images, nuclei are counterstained with DAPI (blue). Dotted lines in B, D, F, G and H delineate the cell soma. Scale bars: 5 μm.

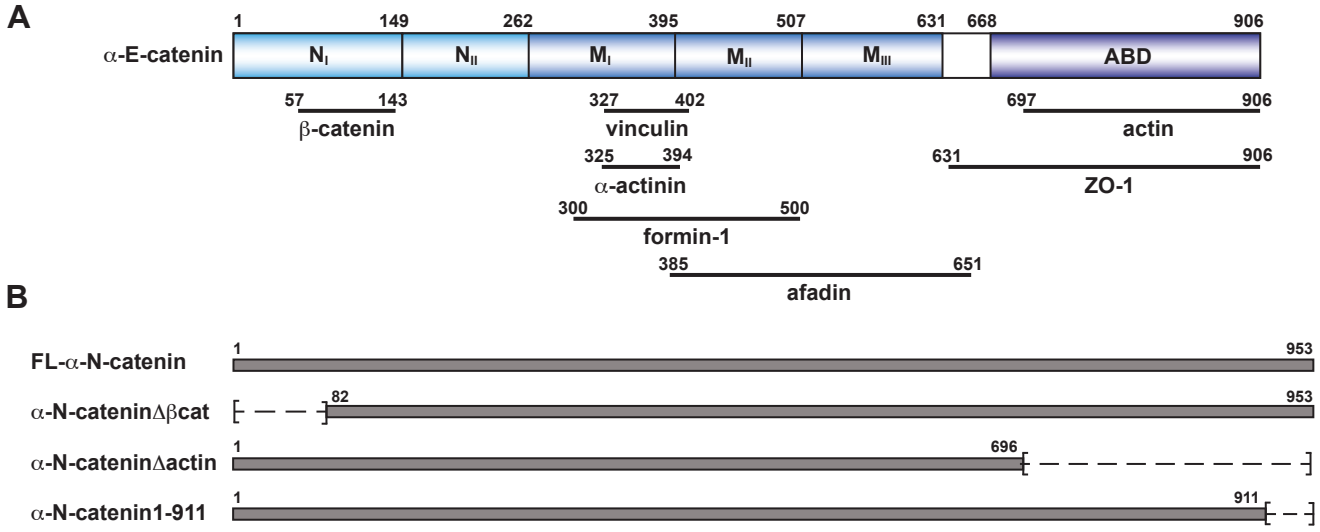

Fig. S5. Interaction domains of α-catenin with some of its binding partners. (A) Diagram of αE-catenin and the binding regions of its interacting partners. The different subdomains of the protein are depicted as boxes (adapted from (Pokutta et al., 2014)), lines and numbers below the protein diagram indicate the regions of αE-catenin that are necessary for its interaction with various partners according to the following references: β-catenin (Pokutta and Weis, 2000); vinculin and ZO-1 (Imamura et al., 1999); α-actinin (Nieset et al., 1997); formin-1 (Kobielak et al., 2004); afadin (Pokutta et al., 2002), and actin (Weiss et al., 1998). NI, NII: four-helix bundles of the N-terminal domain; MI, MII and MIII: four-helix bundles of the middle region; ABD: actin binding domain. **(B)** αN-catenin constructs used in this work. Four different constructs were amplified for electroporation experiments, including the full-length protein and 3 deletion constructs. Deleted regions are indicated by dashed lines and numbered.

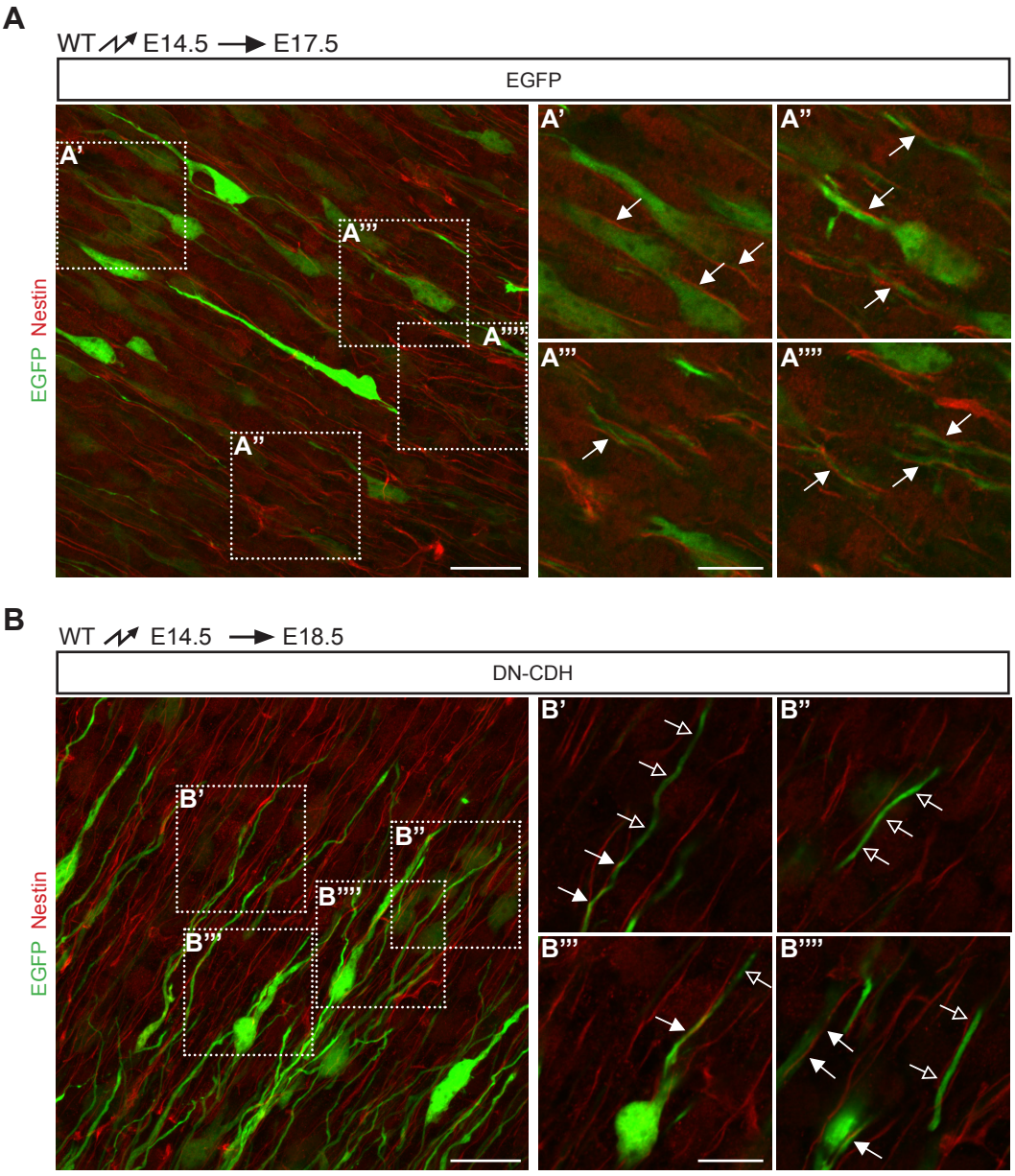

Fig. S6. Alignment of neuronal processes with RGC fibers in control and DN-CDH electroporated neurons . (**A**) Stack of confocal images of neurons expressing EGFP. Panels on the right (A' to A'''') are single confocal sections of the areas boxed in the main image. The soma and leading processes of control electroporated neurons (green) tend to be in close apposition (filled arrows) to nestin-labeled radial glia processes (red). (**B**) Stack of confocal sections of neurons electroporated with DN-CDH. Panels on the right (B' to B'''') are single confocal sections of the areas boxed in the main image. The leading processes of DN-CDH expressing neurons have stretches that do not contact RG processes (empty arrows). Some regions of close contact to RG processes can still be identified (filled arrows). Scale bar: 20 μm (A, B), 10 μm (A'-A'''', B'-B'''').

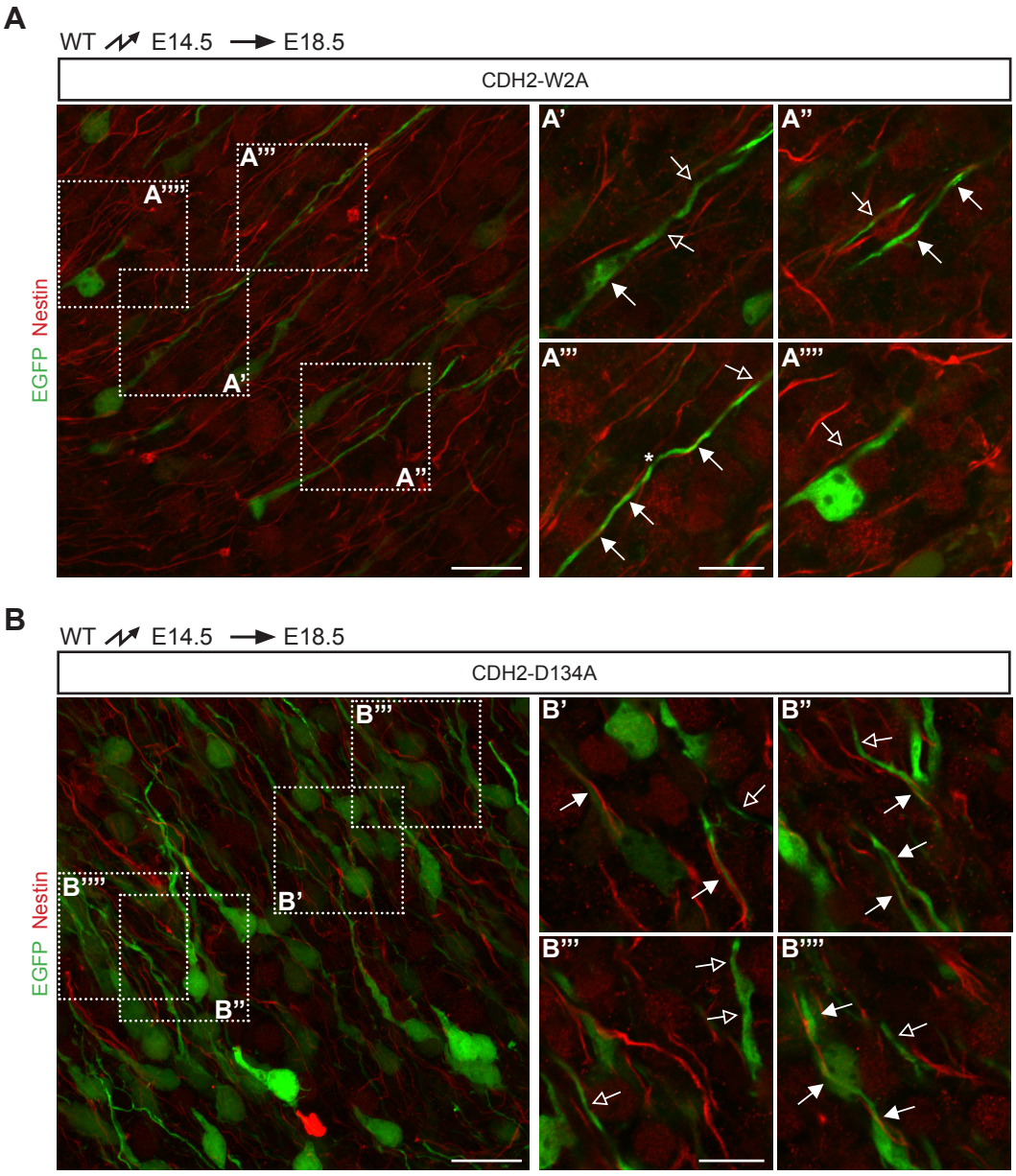

Fig. S7. Alignment of neuronal processes with RGC fibers in neurons expressing adhesion-deficient CDH2. (**A**,**B**) Stack of confocal images of neurons expressing CDH2-W2A (A) or CDH2-D134A (B). Panels on the right (A' to A'''' and B' to B'''') are different single confocal sections of the areas boxed in the main images. The leading processes of neurons expressing adhesion-deficient cadherins do contact RG processes for some stretches (filled arrows) but also show regions of no contact (empty arrows). Asterisk in A''' marks the point where the leading process jumps from one RG process to a different one. Scale bar: 20 μm (A, B); 10 μm (A'-A'''', B'-B'''').

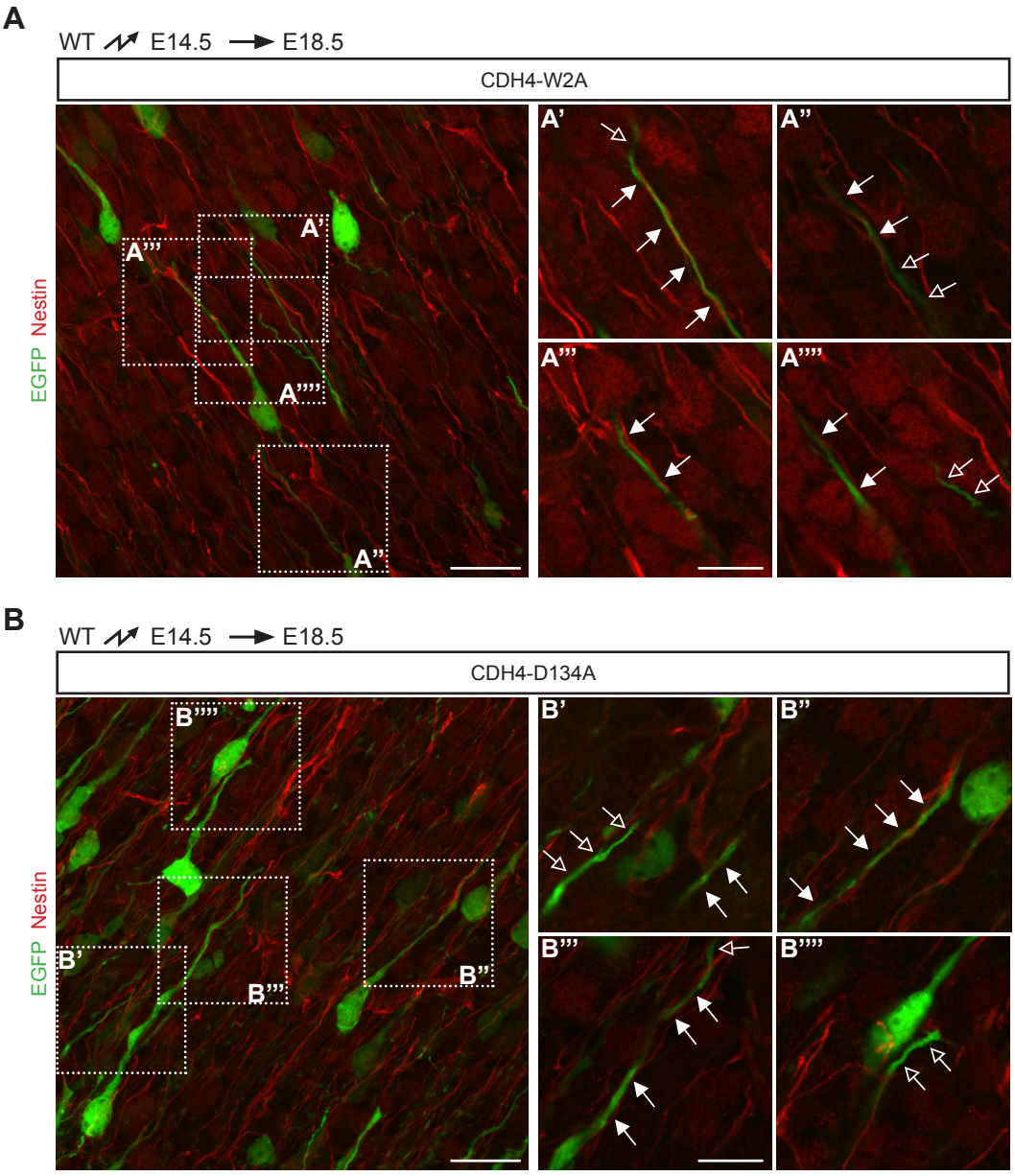

Fig. S8. Alignment of neuronal processes with RGC fibers in neurons expressing adhesion-deficient CDH4. (**A,B**) Stack of confocal images of neurons expressing CDH4-W2A (A) or CDH4-D134A (B). Panels on the right (A' to A'''' and B' to B'''') are different single confocal sections of the areas boxed in the main images. The leading processes of neurons expressing adhesion-deficient cadherins do contact RG processes for some stretches (filled arrows) but also show regions of no contact (empty arrows). Scale bar: 20 μm (A, B), 10 μm (A'-A'''', B'-B'''').

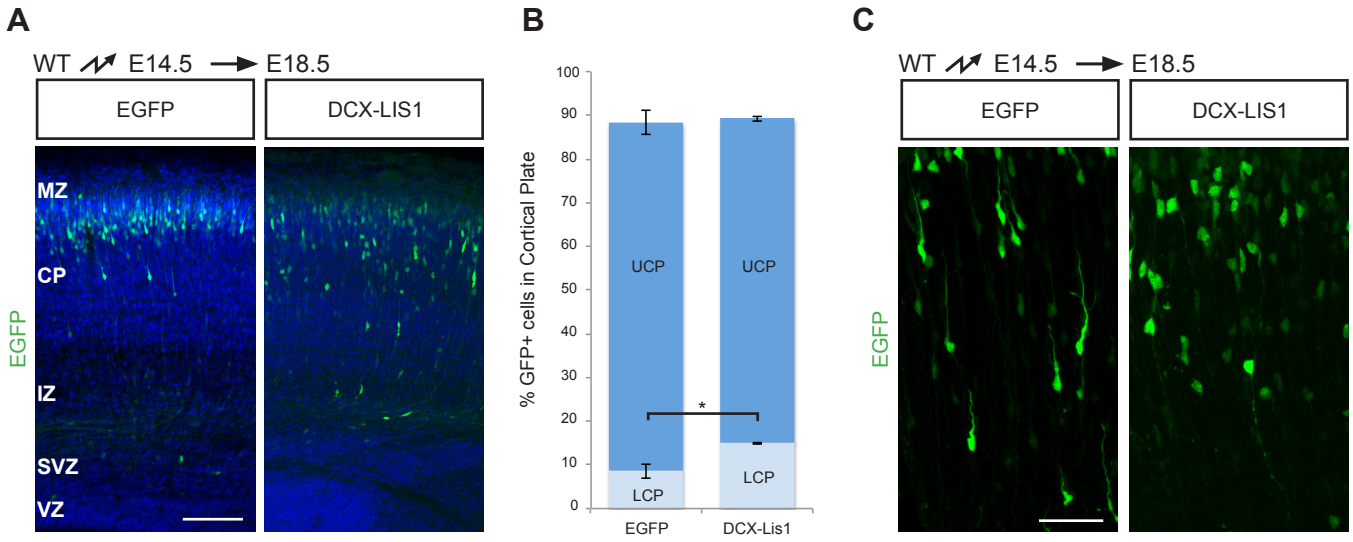

Fig. S9. Lis1 overexpression affects morphology and migration of cortical neurons. (**A**) DCX-Lis1-i-EGFP or a control plasmid were electroporated at E14.5 and brains were analyzed 4 days later. Lis1 overexpressing neurons migrate into the CP in comparable numbers as control neurons, but a higher proportion is still located in the lower half of the CP at E18.5. Electroporated neurons are shown in green, DAPI-stained nuclei in blue. (**B**) Quantification of the percentage of neurons that enter the CP. *p<0.05 for percentage of cells in LCP, difference is not significant for UCP or the CP as a whole. 3 brain slices per brain from 3 different brains were quantified per condition. (**C**) Lis1 overexpression changes the morphology of migrating cortical neurons. Their leading processes are thinner and shorter compared to control neurons. Abbreviations as in Figs 1 and 2. Scale bar: 100 μm (A, C); 50 μm (D).

Table S1. Construct Design. The different cDNAs used in this study were generated by PCR using the indicated primers. cDNAs were verified by sequencing and cloned into the indicated expression vectors.

	Name	Description	Primers used	Cloned into
Cdh constructs	CDH2-FL	Full length Cdh2 (NM_007664.4)	5' AGATCTCTCCGCCTCCATGTGCCGGATAG 3' 5' CTGCAGTGCCGTTCAGTCGTCACCACCG 3'	DCX-iEGFP
	CDH2-W2A	Full length Cdh2 with the aa change W2A	5' AGACGCGGTCATCCCGCCAATCAAC 3' 5' TGACCGCGTCTCTCTTCTGCCTTTG 3'	DCX-iEGFP
	CDH2-D134A	Full length Cdh2 with the aa change D134A	5' CATTGCTGCGGATGATCCAAATGC 3' 5' CCGCAGCAATGGCAGTGACC 3'	DCX-iEGFP
	CDH2-GFP	Full length Cdh2 fused C-terminally to EGFP	5' TGGTGGCGACGTCGTCACCACCGCCGTAC 3' 5' TGGTGACGACGTCGCCACCATGGTGAGCAAG 3'	pCBA
	CDH4-FL	Full length Cdh4 (NM_009867.2)	5' ATTCGTTCGAAGCGGGGACGATGACCACAG 3' 5' CTCCTGCAAATGTGCTTGTGG 3'	DCX-iEGFP
	CDH4-W2A	Full length Cdh4 with the aa change W2A	5' TGACGCGGTCATCCCACCCATCAAC 3' 5' TGACCGCGTCACGCTTCTGTCTCCTC 3'	DCX-iEGFP
	CDH4-D134A	Full length Cdh4 with the aa change D134A	5' CAACGCTGCAGATGATAGCACCAC 3' 5' CTGCAGCGTTGGCTGTGACG 3'	DCX-iEGFP
	DN-CDH	Cdh2 aa 746 to 906	5' AGATCTCTCCGCCTCCATGAAACGGCGGGATAAAGAGCGCCAAG 3' 5' ATCCCGGGCCCGCGGTACCGTC 3' PCR template was Cdh2 cloned into pCIG and the reverse primer is located at the beginning of the IRES sequence. The PCR product was cloned into pGEM-T and then subcloned into DCX-iGFP using EcoRI and XmaI.	DCX-iEGFP
	DN-CDHΔβcat	DN-CDH lacking aa 838 to 862	5' TGGAGCCGCTATTAATGAAGTCCCCAATATCCCCAG 3' 5' CTTCATTAATAGCGGCTCCACGGCTGGCTC3'	DCX-iEGFP
	DN-CDHΔPTP1B	DN-CDH lacking aa 866 to 883	5' GGTAGTCATAGGAGCCGCTGCCCTCGTAGTC 3' 5' CAGCGGCTCCTATGACTACCTGAATGACTGGG 3'	DCX-iEGFP
αNcatenin constructs	pCIG-αNcat	Full length α-N-catenin (NM_001109764.1)	5' AACGCTCGAGACACAGGGAGCATGACTTCGG 3' 5' AAGCAATTGGTCCTAGAAGGAATCCATTGCCTTG 3'	pCIG
	pCIG-αNcatΔactin	α-N-catenin aa 1 to 696	5' AACGCTCGAGACACAGGGAGCATGACTTCGG 3' 5' CCTGAATTCTCACTTGCTTTTTTCTTGGTGGA 3'	pCIG
	pCIG-αNcatΔβcat	α-N-catenin aa 82 to 953	5' AACGCTCGAGACACAGGGAGCATGAGCCAAGACCTCAAAGAAGAG 3' 5' AAGCAATTGGTCCTAGAAGGAATCCATTGCCTTG 3'	pCIG
	pCIG-αNcat1-911	α-N-catenin aa 1 to 911	5' AACGCTCGAGACACAGGGAGCATGACTTCGG 3' 5' AAGCAATTGTTACTAAGGAGCCTTCATCTTCCAAGAC 3'	pCIG
	DN-PTP1B	Full length PTP1B (NM_011201.3) with aa change C215S	5' TCCACAGCAGCGCCGGCATC 3' 5' GCTGCTGTGGACCACAATGG 3'	DCX-iEGFP
Lis1 constructs	LIS1	Full length Lis1 (NM_013625)	5' CTAGAATTCTACAGCCAAAATGGTGCTGTC 3' 5' AATCCGCGGCTATCAACGGCACTCCCACACCTTTAC 3'	DCX-iEGFP
	HA-LIS1	Full length Lis1 with an N-terminal HA tag	5'TCGACTACAGCCAAAATGTACCCATACGATGTTCCAGATTACGCTGTG CTGTCCCAGAGACAACG 3' 5' AATGAATTCCTATCAACGGCACTCCCACACCTTTAC 3'	pCBA
In situ probes	β-catenin	Bases 989 to 1374 of NM_007614.2	5' GCATAATCTCCTGCTCCATCAG 3' 5' GGTTTCTGAGAGTCCAAAGACAG 3'	pGEM-T
	Cdh2	Bases 724 to 1370 of NM_007664.4	5' GGAGGCTTCTGGTGAAATTGC 3' 5' CATGTGCTCTCAAGTGAAACC 3'	pGEM-T
	Cdh4	Bases 259 to 880 of NM_009867.2	5'GGCTACACTGCGTTGATCTCC3' 5'CGTGGGCTCGGAGATGGTAAG3'	pGEM-T
	Cdh6	Bases 1074 to 1497 of NM_007666.3	5' AGGAATGAGCTGAGCCGTTCG 3' 5' CGGGGGTCTTAAACTGGTAGG 3'	pGEM-T
	Cdh11	Bases 2007 to 2627 of NM_009866.4	5' CACCCCAAGGCACTCTCCAAC 3' 5' CCCAGGTCTAGGCATATACTGATAC 3'	pGEM-T
	Cdh13	Bases 220 to 961 of NM_019707.4	5' CCTGCCGAATTCATCGAGGAC 3' 5' GACGGATGTTGTACCTCAGGAG 3'	pGEM-T
Markers	Golgi marker	First 338 bases of human GalNacT2 fused to dsRedEx	5' ACTGCTCGAGGCCGCCACCATGCGGCGGCGCTCGCGGATG 3' 5' GGAGGCCATAGCTGCTACTCGAAGCTTATCACTCTCCACCTGG 3'	pCBA
	Centrosomal marker	Kind gift from Dr Song-Hai Shi		
	Actin-GFP	Addgene Plasmid 21948		

Table S2. Antibodies used in this study. Antibodies were purchased from the indicated vendors and used at the stated dilutions.

Antibody	Dilution	Company	Reference
anti-CDH2 (6B3) rat monoclonal	1:200	Developmental Studies Hybridoma Bank, NICHD and University of Iowa Department of Biology	6B3, deposited by Knudsen, K.A.
anti-CDH2 (GC-4) mouse monoclonal	1:200	Sigma-Aldrich, St. Louis, Missouri, United States	C3865
anti-CDH4 (MRCD5) rat monoclonal (1:200)	1:200	Developmental Studies Hybridoma Bank, NICHD and University of Iowa Department of Biology	MRCD5, deposited by Takeichi, M. / Matsunami, H.
anti-Nestin (Rat401) mouse monoclonal	1:20	Developmental Studies Hybridoma Bank, NICHD and University of Iowa Department of Biology	Rat-401, deposited by Hockfield, S.
anti-Nestin rabbit polyclonal	1:200	Abcam	ab27952
anti-HA (clone HA-7) mouse monoclonal	1:100	Sigma-Aldrich, St. Louis, Missouri, United States	H9658
Anti-HA (clone 3F10) rat monoclonal	1:500	Sigma-Aldrich, St. Louis, Missouri, United States	000000011867423001
anti-Pax6 rabbit polyclonal	1:300	Biolegend, San Diego, California, United States	901301
anti-neuronal Class III β-Tubulin (clone Tuj1) mouse monoclonal	1:2000	Biolegend, San Diego, California, United States	801201

Supplemental references

Imamura, Y., Itoh, M., Maeno, Y., Tsukita, S. and Nagafuchi, A. (1999). Functional domains of alpha-catenin required for the strong state of cadherin-based cell adhesion. *J Cell Biol* **144**, 1311–1322.

Kobielak, A., Pasolli, H. A. and Fuchs, E. (2004). Mammalian formin-1 participates in adherens junctions and polymerization of linear actin cables. *Nat Cell Biol* **6**, 21–30.

Pokutta, S. and Weis, W. I. (2000). Structure of the dimerization and beta-catenin-binding region of alpha-catenin. *Mol Cell* **5**, 533–543.

Pokutta, S., Choi, H.-J., Ahlsen, G., Hansen, S. D. and Weis, W. I. (2014). Structural and Thermodynamic Characterization of Cadherin-β-catenin-α-catenin Complex Formation. *J Biol Chem*.

Pokutta, S., Drees, F., Takai, Y., Nelson, W. J. and Weis, W. I. (2002). Biochemical and structural definition of the l-afadin- and actin-binding sites of alpha-catenin. *J Biol Chem* **277**, 18868–18874.

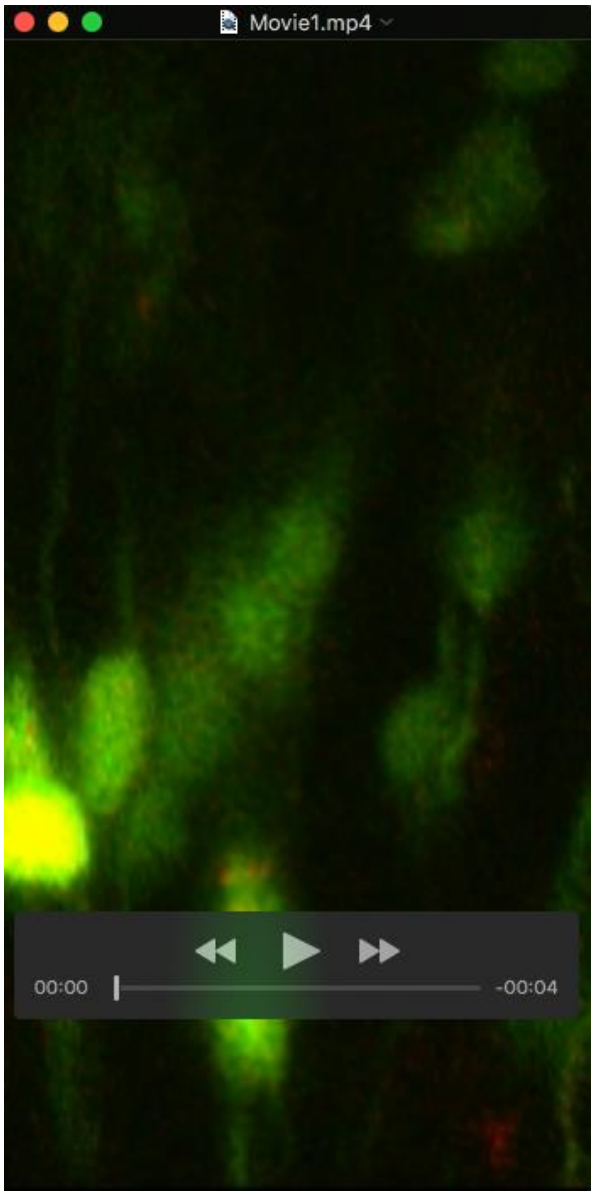

Supplementary Movie 1
Normal centrosomal and nuclear movement in a control neuron migrating by glia-guided locomotion.

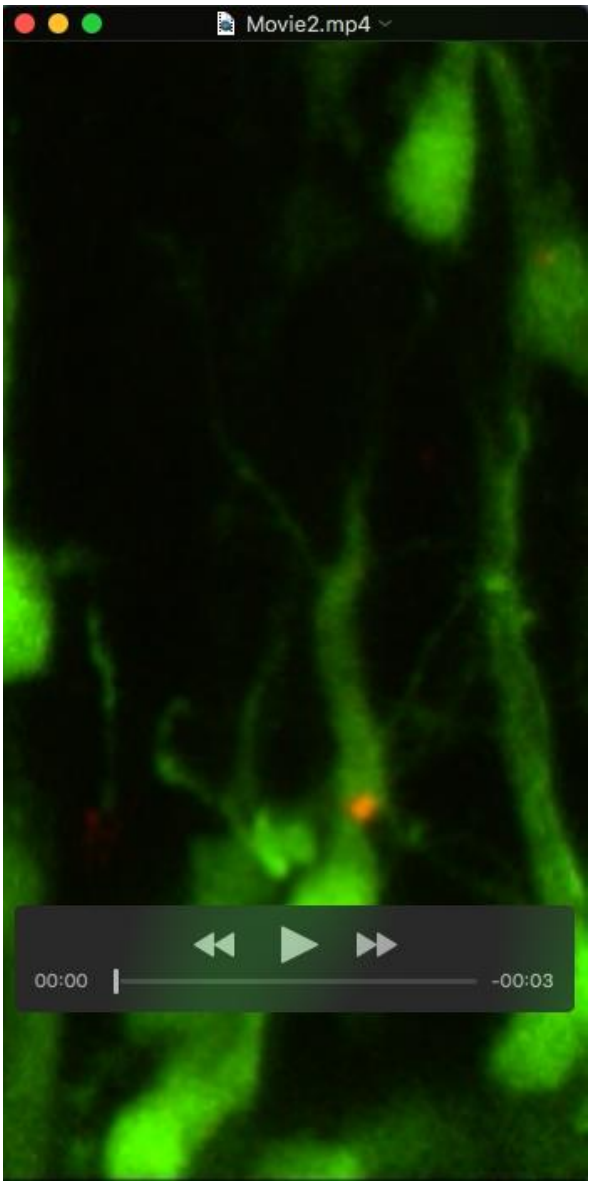

Supplementary Movie 2
Arrested centrosomal and nuclear movement in a neuron expressing DN-CDH.

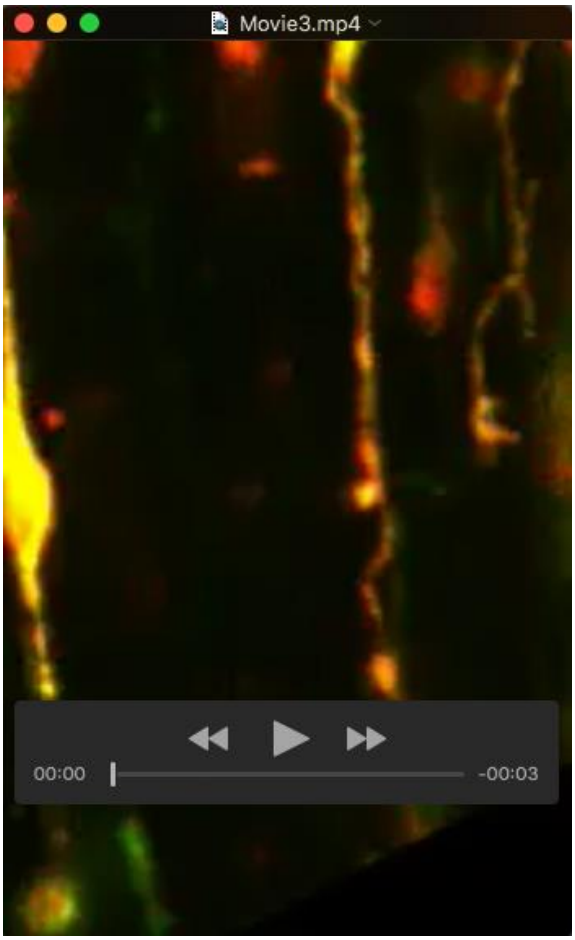

Supplementary Movie 3
Actin dynamics in a control neuron migrating by glia-guided locomotion.

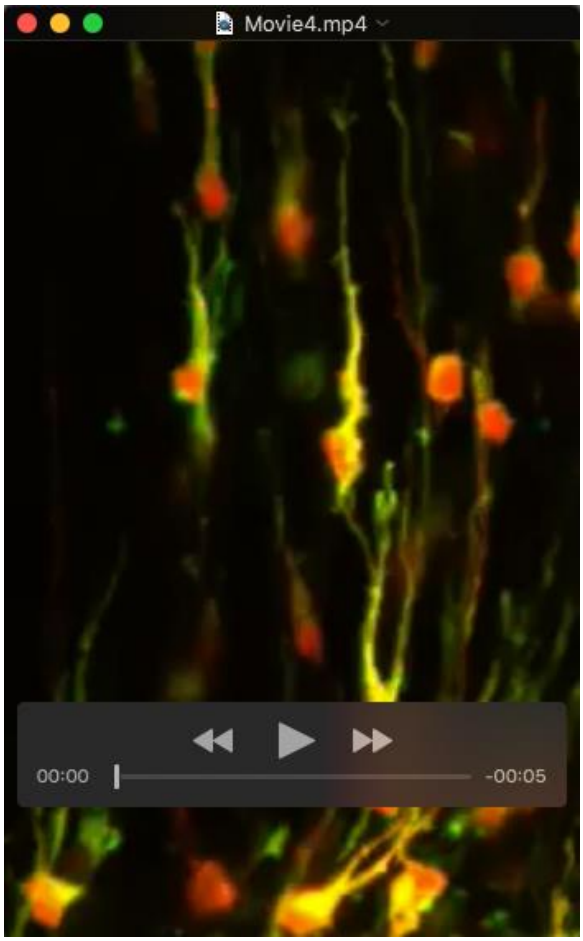

Supplementary Movie 4
Actin dynamics in a neuron expressing CDH2-D134A.

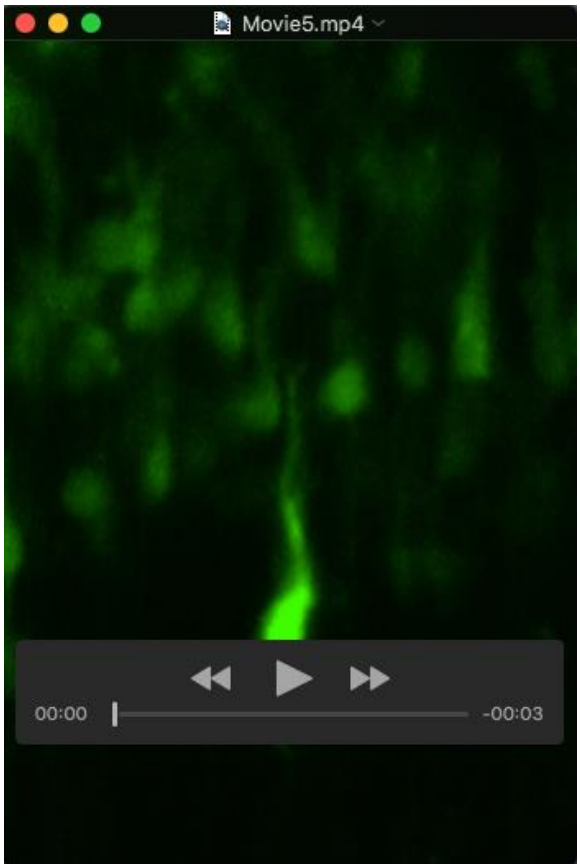

Supplementary Movie 5
Nuclear translocation after Calyculin A treatment in a control neuron.

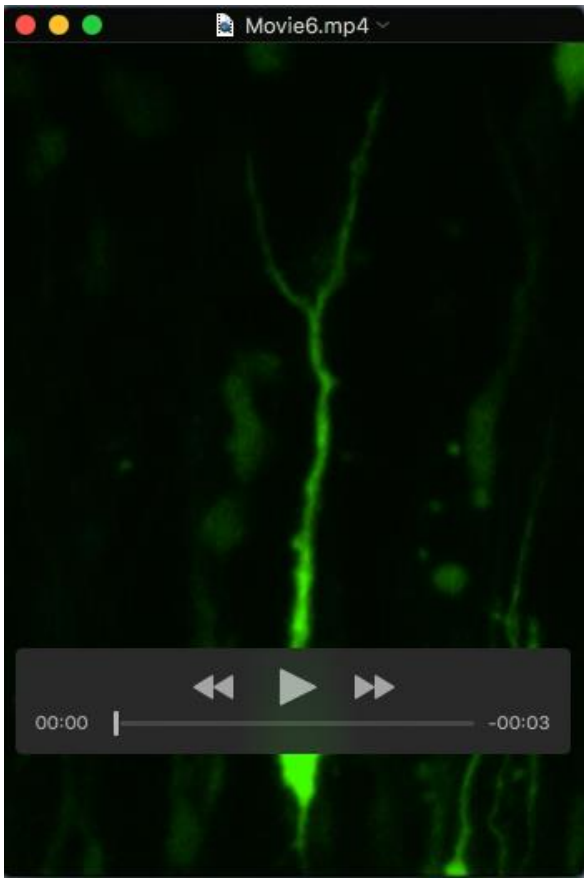

Supplementary Movie 6
Leading process retraction after Calyculin A treatment in a neuron expressing DN-CDH.